Active thermography signal processing techniques for defect detection and characterization on composite materials

C. Ibarra-Castanedo[a], N. P. Avdelidis[b], M. Grenier[a], X. Maldague[a] and A. Bendada[a]

[a]Computer Vision and Systems Laboratory, Department of Electrical and Computer Engineering, Laval University, Quebec City, Canada, G1V 0A6, {IbarraC, Bendada, MaldagX}@gel.ulaval.ca.
[b]National Technical University Of Athens, School of Chemical Engineering, Materials Science & Engineering Section, Zografou Campus, Athens, Greece 15780.

ABSTRACT

Active thermography has been extensively investigated in the past few years for the nondestructive evaluation of different types of materials. Composites in particular have received considerable attention given that active thermography has shown to be well suited for the detection and characterization of most kinds of defects typically found in these materials such as impact damage, delaminations, disbonds and inclusions. Signal processing is a necessary step of the inspection process, especially if defect characterization is required. A wide variety of techniques have been developed from the classical thermal-based techniques to signal transformation algorithms (adapted from the area of machine vision) on which temporal data is transformed to a different domain (frequency, Hough, principal components, Laplace, high-order moments, etc.) with the purpose of simplifying data analysis. In this paper, a review of some of these processing techniques is presented and exemplified using a Kevlar® panel and a GLARE specimen.

Keywords: active infrared thermography, signal processing, composites, pulsed thermography.

1. ACTIVE THERMOGRAPHY

1.1. Excitation sources

Active infrared thermography [1] is a nondestructive testing and evaluation (NDT&E) technique requiring an external source of energy to induce a temperature difference between defective and non-defective areas in the specimen under examination. A wide variety of energy sources are available, the most common types can be divided into *optical*, *mechanical* or *inductive*, although many other sources can be employed.

Optical excitation

With optical excitation, defects are stimulated *externally*, that is, the energy is delivered to the surface of the specimen, where light is transformed into heat. Thermal waves propagate by conduction from the surface through the specimen until they reach an internal discontinuity that either slows down or speeds up their propagation (depending on the thermal properties of both the specimen and the discontinuity). This can be seen as *hot* or *cold* spots on the specimen's surface with an infrared camera. Optical devices include photographic flashes (for pulsed heat stimulation), infrared lamps (for step heating) or halogen lamps (for periodic heating), among others. This is the most widely used form of excitation in thermography for NDT&E [2]. It was originally used to develop the classical thermographic techniques, *pulsed* and *lock-in* thermography, described in section 2.

Mechanical excitation

In the case of mechanical excitation, the energy is applied into the specimen by means of mechanical oscillations using, for example, a *sonic* or *ultrasonic* transducer that is in contact with the specimen (usually a coupling media is employed). In this case, the defects are stimulated *internally*; the mechanical oscillations transmitted into the specimen spread in all directions inside it. The mechanical energy is dissipated at the discontinuities in the form of heat waves that travel to the surface by conduction.

Ultrasonic excitation has received considerable attention in recent years. The technique known as *vibrothermography* (also *ultrasound thermography* [3] or *thermosonics* [4]) is typically used in the inspection of cracks and micro-cracks [5]

Thermosense XXXII, edited by Ralph B. Dinwiddie, Morteza Safai, Proc. of SPIE
Vol. 7661, 76610O · © 2010 SPIE · CCC code: 0277-786X/10/$18 · doi: 10.1117/12.850733

in metallic structures, which are very difficult to inspect by optical means. As in optical excitation, pulsed thermography (better known as *burst* thermography in the case of ultrasonic excitation) and lock-in thermography are used.

Inductive excitation

Inductive excitation can be applied *internally* to electro-conductive-materials, generating eddy currents at a specific depth (determined by the frequency of the excitation), heating up the specimen and the eventual internal defects. Surface or subsurface defects produce variations on the eddy current patterns, changing the temperature distribution. As with the previous excitation forms, these temperature variations can be detected on the surface with an infrared camera.

Eddy current thermography [6] or *Induction heating thermography* [7] is the latest development in the field of active thermography. It is receiving considerable attention at the moment (year 2008) from researchers around the world [8, 9]. As in the case of optical and mechanical excitation, inductive stimulation can be deployed in the form of pulses (pulsed thermography) or amplitude modulations (lock-in thermography), which are discussed in section 2.

Regardless of the excitation mode being used, there are basically three thermographic techniques: pulsed, step and lock-in. The experimental and theoretical aspects are different for each of these techniques and so are the typical applications.

1.2. Experimental configurations

Pulsed thermography

Pulsed thermography (PT) is one of the most popular thermal stimulation methods in active thermography [1, 2]. One reason for this is the quickness of the inspection relying on a short thermal stimulation pulse, with duration going from a few milliseconds for high conductivity material inspection (such as metal) to a few seconds for low conductivity specimens (such as plastics). In addition, the brief heating prevents damage to the component.

Depending on the excitation source, it might be interesting to observe both the heating phase (while the pulse is applied) and the cooling phase, or only the surface cooling phase. For instance, in optical PT there is no interest in observing the thermal changes during the excitation since these images are often saturated. More importantly, this early data does not contain any information about the internal defects yet. However, images prior to the excitation (*cold image*s) are very useful at pre-processing stages and for some advanced processing techniques. Conversely, thermal changes in vibrothermography are very fast – a few seconds – and important information can be found at any instant, during heating or cooling. In this case, the whole profile needs to be analyzed.

Step heating thermography

Step heating uses a larger pulse (from several seconds to a few minutes). The temperature decay is of interest; in this case, the increase of surface temperature is monitored during the application of a step heating pulse. Variations of surface temperature with time are related to specimen features as in PT. This technique is sometimes referred to as time-resolved infrared radiometry (TRIR). TRIR finds many applications such as evaluation of coating thickness – including multilayered coatings, determination of coating-substrate bond integrity or evaluation of composite structures [10]. Although at the moment only optical excitation has been used in step heating, there is no limitation to the use of other excitation forms.

Lock-in thermography

In lock-in thermography (LT) [11], also known as *modulated thermography* [12], the specimen is stimulated with a periodic energy source. Typically, sinusoidal waves are used, although it is possible to use other periodic waveforms. Internal defects, acting as barriers for heat propagation, produce changes in *amplitude* and *phase delay* of the response signal at the surface. Different techniques have been developed to extract the amplitude and phase information. Fourier analysis is the preferred processing technique since it provides single images, *ampligrams* or *phasegrams* (the weighted average of all the images in a sequence). The resulting Signal-to-Noise Ratio (SNR) is therefore very high. Phase data in particular is very interesting in NDT&E [13] as it is less affected than raw thermographic data by non-uniform heating, emissivity variations at the surface, reflections from the environment and surface geometry [14].

Next section presents a review of some of the most interesting signal processing techniques that can be used for the active thermography inspection of composite materials.

2. PROCESSING TECHNIQUES

2.1. Differential absolute contrast (DAC)

Thermal contrast is a basic operation that despite its simplicity is at the origin of many PT algorithms. Various thermal contrast definitions exist [2] but they all share the need for specifying a sound area S_a, *i.e.* a non-defective region. For instance, the absolute thermal contrast $\Delta T(t)$ is defined as [2]:

$$\Delta T(t) = T_d(t) - T_{S_a}(t) \tag{1}$$

with $T_d(t)$ the temperature of a pixel or the average value of a group of pixels on a defective area at time t, and $T_{Sa}(t)$ the temperature at time t for the S_a. No defect can be detected at a particular t if $\Delta T(t)$=0. In practice however, raw data is contaminated with noise and other signal degradations [2] and a threshold of detectability needs to be established.

The main drawback of classical thermal contrast is establishing S_a, especially if automated analysis is needed. Even when S_a definition is straightforward, considerable variations on the results are observed when changing the location of S_a [15].

In the differential absolute contrast (DAC) method [16], instead of looking for a non-defective area, an ideal S_a temperature at time t is computed locally assuming that on the first few images (at least one image at time t' in particular, see below) this local point behaves as a S_a in accordance to Eq. (1), *i.e.* there is no visible defect. The first step is to define t' as a given time value between the instant when the pulse has been launched, and the precise moment when the first defective spot appears on the thermogram sequence, *i.e.* when there is enough contrast for the defect to be detected. At t', there is no indication of the existence of a defect yet, therefore, the local temperature for a S_a is exactly the same as for a defective area [16]:

$$T_{S_a}(t') = T(t') = \frac{Q}{e\sqrt{\pi t'}} \quad \Rightarrow \quad \frac{Q}{e} = \sqrt{\pi t'} \cdot T(t') \tag{2}$$

From this result, T_{Sa} can be computed for every pixel at time t. Substituting Eq. (2) into the absolute contrast definition, *i.e.* Eq. (1) it follows that [16]:

$$\Delta T_{DAC} = T_d(t) - \sqrt{\frac{t'}{t}} \cdot T(t') \tag{3}$$

Actual measurements diverge from the solution provided by Eq. (3) as time elapses and also as the plate thickness increases with respect to the non-semi-infinite case. Nevertheless, the DAC technique has proven to be very efficient by reducing artifacts from non-uniform heating and surface geometry and providing a good approximation even for the case of anisotropic materials at early times [17]. Originally, proper selection of t' required an iterative graphical procedure, for which a graphical user interface was developed [18]. An automated algorithm is also available [19]. Furthermore, a modified DAC technique based on a finite plate model and the thermal quadrupoles theory has been developed as well [20]. The solution includes the plate thickness L explicitly in the solution, extending in this way the validity of the DAC algorithm to later times.

2.2. Thermogaphic signal reconstruction (TSR)

Thermographic signal reconstruction (TSR) [21] is an attractive technique that allows increasing spatial and temporal resolution of a sequence, while reducing at the same time the amount of data to be manipulated. TSR is based on the assumption that temperature profiles for non-defective pixels should follow the decay curve given by the one-dimensional solution of the Fourier equation, *i.e.* Eq. (1), which may be rewritten in the logarithmic form as:

$$\ln(\Delta T) = \ln\left(\frac{Q}{e}\right) - \frac{1}{2}\ln(\pi t) \tag{4}$$

As stated before, Eq. (1) is only an approximation of the solution for the Fourier equation. To fit the thermographic data, Shepard 2001 proposed to use a p-degree polynomial of the form [22]:

$$\ln(\Delta T) = a_0 + a_1 \ln(t) + a_2 \ln^2(t) + \ldots + a_p \ln^p(t) \tag{5}$$

Thermal profiles corresponding to non-defective areas in the sample will follow an approximately linear decay, while the thermal behavior of a defective area will diverge from linearity. Typically, p is set to 4 or 5 to avoid "ringing" and insure a good correspondence between acquired data and fitted values. At the end, the entire raw thermogram sequence is reduced to p+1 coefficient images (one per polynomial coefficient) from which synthetic thermograms can be reconstructed.

Synthetic data processing brings interesting advantages such as: significant noise reduction, possibility for analytical computations and data compression (from N to p+1 images). Analytical processing becomes also possible, giving the possibility of estimating the actual temperature for a time between acquisitions from the polynomial coefficients. Furthermore, calculation of first and second time derivatives from the synthetic coefficients is straightforward. First time derivatives indicate the rate of cooling while second time derivatives refer to the rate of change in the rate of cooling. Therefore, time derivatives are more sensitive to temperature changes than raw thermal images. There are no purpose using higher order derivatives, since, besides the lack of a physical interpretation, no defect contrast improvement can be observed. Finally, TSR synthetic data can be used in combination with other algorithms to perform quantitative analysis as described at the end of the next section.

2.3. Principal component thermography (PCT)

As explained above, the Fourier transform provides a valuable tool to convert the signal from the temperature-time space to a phase-frequency space but it does so through the use of sinusoidal basis functions, which may not be the best choice for representing transient signals, which are the temperature profiles typically found in pulsed thermography. Singular value decomposition (SVD) is an alternative tool to extract spatial and temporal data from a matrix in a compact or simplified manner. Instead of relying on a basis function, SVD is an eigenvector-based transform that forms an orthonormal space. SVD is close to principal component analysis (PCA) with the difference that SVD simultaneously provides the PCAs in both row and column spaces.

The SVD of an MxN matrix $\mathbf{A}$ ($M>N$) can be calculated as follows [23]:

$$\mathbf{A}=\mathbf{U}\mathbf{R}\mathbf{V}^{\mathrm{T}} \tag{6}$$

where $\mathbf{U}$ is a MxN orthogonal matrix, R being a diagonal NxN matrix (with singular values of $\mathbf{A}$ present in the diagonal), $\mathbf{V}^{\mathbf{T}}$ is the transpose of an NxN orthogonal matrix (characteristic time).

Hence, in order to apply the SVD to thermographic data, the 3D thermogram matrix representing time and spatial variations has to be reorganised as a 2D MxN matrix $\mathbf{A}$. This can be done by rearranging the thermograms for every time as columns in $\mathbf{A}$, in such a way that time variations will occur column-wise while spatial variations will occur row-wise. Under this configuration, the columns of $\mathbf{U}$ represent a set of orthogonal statistical modes known as empirical orthogonal functions (EOF) that describes spatial variations of data [23, 24]. On the other hand, the principal components (PCs), which represent time variations, are arranged row-wise in matrix $\mathbf{V}^{\mathbf{T}}$. The first EOF will represent the most characteristic variability of the data; the second EOF will contain the second most important variability, and so on. Usually, original data can be adequately represented with only a few EOFs. Typically, a 1000 thermogram sequence can be replaced by 10 or less EOFs.

The 4 techniques just described are intended to process PT data. As discussed next, lock-in thermography signals behave differently.

2.4. Pulsed phase thermography (PPT)

Pulsed phase thermography (PPT) [25, 26] is another interesting technique, in which data is transformed from the time domain to the frequency domain using the one-dimensional discrete Fourier transform (DFT) [25]:

$$F_n = \Delta t \sum_{k=0}^{N-1} T(k\Delta t) \exp^{(-j2\pi nk/N)} = \mathrm{Re}_n + j\,\mathrm{Im}_n \tag{7}$$

where j is the imaginary number (j_2=-1), n designates the frequency increment (n=0,1,…N), Δt is the sampling interval, and Re and Im are the real and the imaginary parts of the transform, respectively.

In this case, real and imaginary parts of the complex transform are used to estimate the amplitude A, and the phase ϕ [25]:

$$A_n = \sqrt{\mathrm{Re}_n^2 + \mathrm{Im}_n^2} \quad \text{and} \quad \phi_n = \tan^{-1}\left(\frac{\mathrm{Im}_n}{\mathrm{Re}_n}\right) \tag{8}$$

The DFT can be used with any waveform (*e.g.* transient pulsed thermographic profiles). Phase profiles for surface temperature are anti-symmetric, providing redundant information in both sides of the frequency spectra. In the following, only the positive part of the frequency spectra is used whilst the negative frequencies can be safely discarded.

The phase is of particular interest in NDE given that it is less affected than raw thermal data by environmental reflections, emissivity variations, non-uniform heating, and surface geometry and orientation. These phase characteristics are very attractive not only for qualitative inspections but also for quantitative characterization of materials. For instance, a depth inversion technique using the phase from PPT has been proposed [27]. The technique relies on the thermal diffusion length equation, *i.e.* $\mu=(\alpha/\pi \bullet f)^{1/2}$, in a manner similar to lock-in thermography (LT) [28]. The depth of a defect can be calculated from a relationship of the form [27]:

$$z = C_1 \cdot \mu = C_1 \sqrt{\frac{\alpha}{\pi \cdot f_b}} \tag{9}$$

where f_b [Hz] is the blind frequency defined as the limiting frequency at which a defect located at a particular depth presents enough (phase or amplitude) contrast to be detected on the frequency spectra.

2.5. Higher order statistics thermography (HOST)

The most commonly employed statistic parameters are measures of central tendency and variability, with the mean and the variance being the most representative ones. Theoretically, only the first four statistic parameters have a physical definition in the mathematical study of distribution. These are the mean, variance, skewness and kurtosis, corresponding to the first, second, third and fourth statistical moments respectively. The mean μ is the average score in a distribution and the variance σ^2, the second central moment of a distribution, is a measure of statistical dispersions about the mean of the distribution. These two parameters can be expressed as, respectively [29]:

$$\mu = E[X] = \frac{1}{P}\sum_{n=1}^{P} X_n \quad \text{and} \quad \sigma^2 = E\left[\left(X - E[X]\right)^2\right] \tag{10}$$

The standardized central moments M_I, where the subscript I indicates the moment order, can be defined as:

$$M_I = \frac{E\left[\left(X - E[X]\right)^I\right]}{\sigma^I} \tag{11}$$

Skewness is the third standardized central moment (I=3), it represents a measure of symmetry, or more precisely, the lack of symmetry of a distribution. Kurtosis is the fourth moment (I=4) and it characterizes the relative flatness of a distribution in relation to the shape of a normal distribution. Standardized central moments of higher-order present large values due to the high power terms involved in their calculations and it cannot often be defined physically. They are associated to the presence of outliers in the distribution.

In order to take advantage of HOS for active thermography, the histogram distributions of the thermal profiles can be reconstructed. Histograms for pulsed thermographic thermal profiles do not have a normal distribution. All distributions are asymmetrical and skewed to right, *i.e.* they are positively skewed and their skewness parameter has a positive value. Nevertheless, the skewness value increases with the defect depth and is the highest for non-defective areas. Hence, the skewness value of a data distribution obtained from the surface temperature evolution depends on both the subsurface defect presence and its depth [30]. It is therefore possible to obtain a HOS map, *i.e.* a single image, providing an indication about the presence or no-presence of defects and the relative depths.

Next section presents some comparative examples showing the potential of these techniques for the inspection of composite materials.

3. COMPARATIVE EXAMPLES

3.1. Kevlar® standard panel

The Kevlar® panel shown in Figure 1b. contains 16 Teflon® inserts distributed at different locations as indicated. The specimen was inspected in two parts: regions I and II, delimited in Figure 1b.

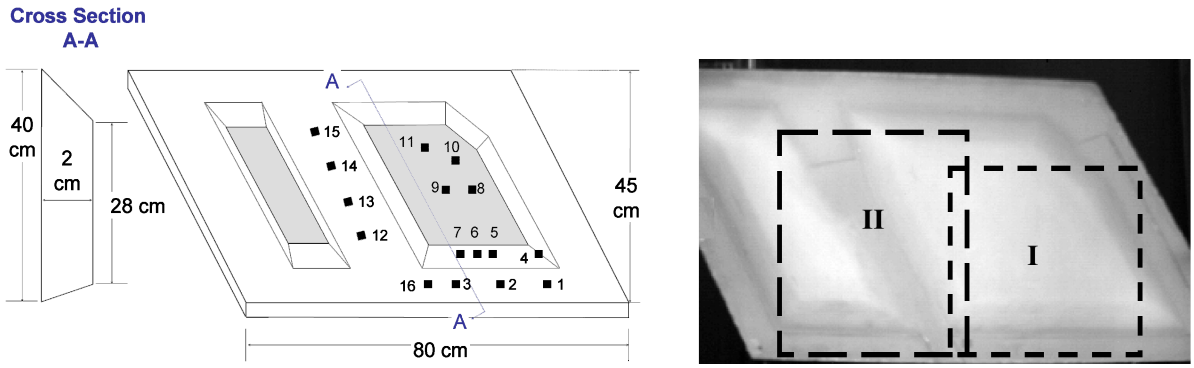

(a) **(b)**

Figure 1. Kevlar® panel: (a) Schematic illustration showing defect locations, (b) raw temperature thermogram (first image after flash heating) showing the two inspected areas (Region I and Region II).

The raw thermogram 355 ms after the flash (Figure 2a) reveals the presence of 5 of 10 defects present in region I, *i.e.* defects 3, 6, 7, 11 and 16. DAC processing (Figure 2b) allows detecting these same defect and defect 10 as well. Defect 2 is visible in the first (Figure 2c) and second (Figure 2d) derivative images at 177 ms with increased contrast (although defect 6 is not clearly seen in Figure 2d). Although the non-planar shape of the surface is still seen, processing results with DAC and TSR greatly improves the defect contrast. For region II, the DAC result (Figure 2e) provides the best overall contrast, revealing the presence of the four defects.

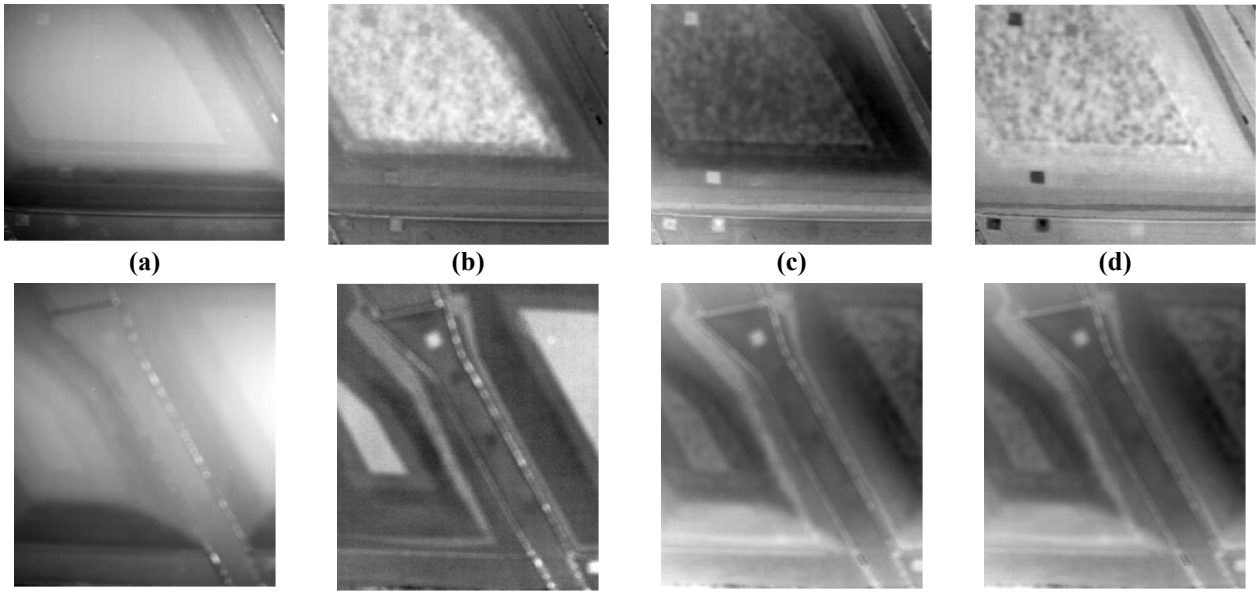

(a) **(b)** **(c)** **(d)**

(e) **(f)** **(g)** **(h)**

Figure 2. Results for region I: (a) raw temperature at t=355 ms, (b) DAC at t=532 ms; (c) first and (d) second derivatives at t=177 ms. Region II: (e) raw temperature at t=355ms; (f) DAC at t=355 ms; (g) first and (h) second time derivatives at t=177 ms.

3.2. Delaminations in GLARE

An schematic illustration of a GLARE specimen containing 31 fabricated defects (film release) as indicated, is shown in Figure 3a. A photograph of the rear side of the specimen can be seen in Figure 3b. The GLARE plate was inspected by pulsed thermography from both sides and data was processed using different techniques.

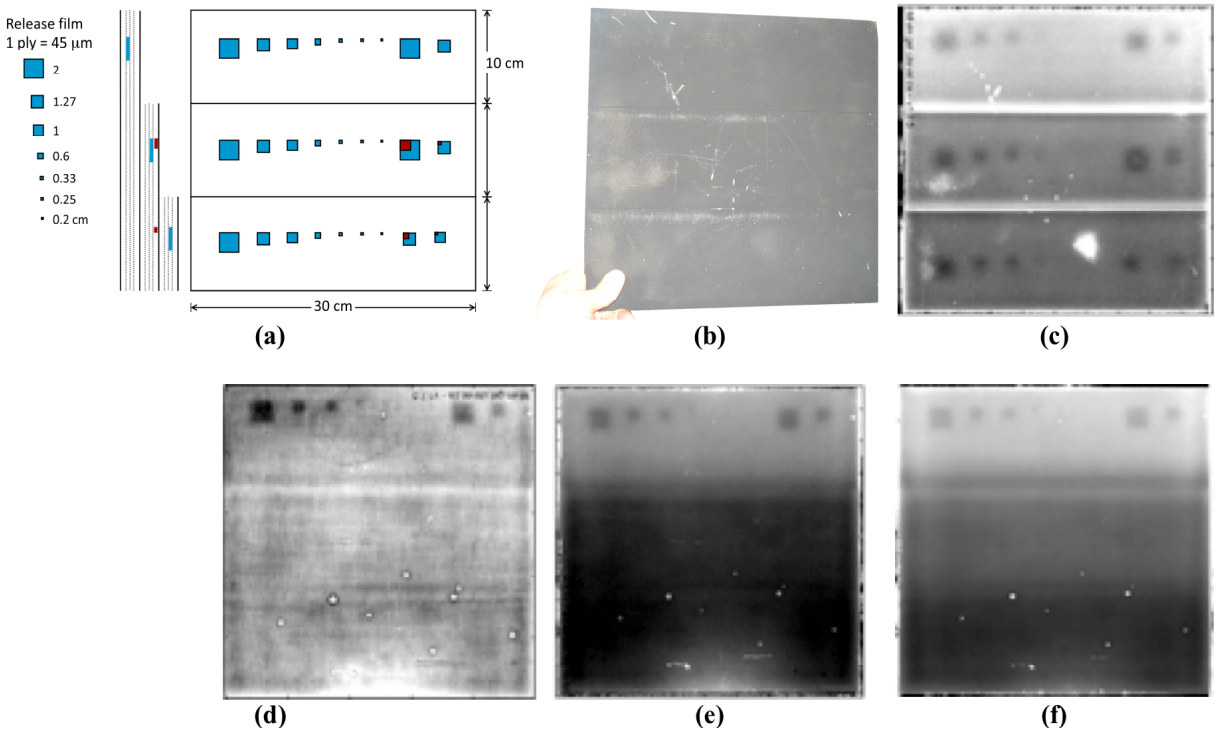

Figure 3. GLARE specimen: (a) Schematic representation showing defect sizes and location, (b) photograph of the specimen, (c) PPT phasegram at f=0.52 Hz (inspected from the back side), (d) EOF5 from 1st derivative (inspected from the front side), (e) PPT phasegram at f=0.44 Hz (inspected from the front side), and (f) skewness image (inspected from the front side).

For instance, Figure 3c shows a phasegram (f=0.52 Hz) obtained by inspecting the sample from the rear side (from the right in Figure 3a) and processing data by pulsed phase thermography. The fifteen (15) largest defects can be seen in this image. Two (2) smaller defects can also be seen with lesser contrast. An artifact (reflection from the flashes, can also be seen, even though the surface of the sample was blackpainted to reduce reflections. PPT was selected to reduce reflections even further. Still, this kind of artifact can still be seen.

The specimen was also tested by PT from the front side (from the left in Figure 3a). Only the 6 largest defects of the top section (see Figure 3a), having just 1 layer of aluminum and 1 layer of glass fiber, can be clearly identified as seen in the EOF5 obtained by PCT in Figure 3d. As can be seen, although defects clearly appear in this image, no distinction can be observed between sections having more composite layers. On the other hand, the PPT phasegram (f=0.44 Hz) in Figure 3e besides showing the defects it provides as well an indication of a greater number of layer in the mid and bottom sections of the plate (with no distinction between these two). Finally, the skewness image show the same defects and also provide a good indication of the two different layer composition of the three plate sections.

4. CONCLUSIONS

Several thermographic signal-processing techniques have been implemented over the years. These techniques constitute a valuable tool for improving defect detection and eventually defect characterization. The comparative examples

presented herein for pulsed thermography testing demonstrate that is indeed possible to implement such techniques for the NDT&E of composites.

ACKNOWLEDGEMENTS

Authors want to thank the support of the Chaire de recherché du Canada (MIVIM), the Ministère du développement économique, innovation et exportation du Québec.

REFERENCES

1. Nondestructive Handbook, Infrared and Thermal Testing, Volume 3, X. Maldague technical ed., P. O. Moore ed., 3rd edition, Columbus, Ohio, ASNT Press, 2001, 718 p.
2. Maldague X. P. *Theory and practice of infrared technology for nondestructive testing*, John Wiley & Sons, N. Y. 2001.
3. Dillenz A., Zweschper T. and Busse G. "Progress in ultrasound phase thermography," *Proc. SPIE - The International Society for Optical Engineering, Thermosense XXVIII*, Orlando, FL, 2001*,* Eds. A. E. Rozlosnik and R. B. Dinwiddie, **4360**:574-579.
4. Favro L. D., Han X., Ouyang Z., Sun G., Sui H. and Thomas R. L. "Infrared imaging of defects heated by a sonic pulse," *Rev. Sci. Instr*., 2000.
5. Piau J-M., Bendada A., Maldague X. P. and Legoux J-G. "Nondestructive inspection of open micro-cracks in thermallysprayed-coatings using ultrasound excited vibrothermography," *SPIE - The International Society for Optical Engineering, Thermosense XXIX*, Orlando, FL, April 9-13 2007*,* Eds. K. M. Knettel, V. Vavilov and J. J. Miles, **6541**:654112.
6. Riegert G., Zweschper T., and Busse G. "Eddy-current lockin-thermography: Method and its potential," *Journal de Physique IV*, vol. 125, Jun. 2005, pp. 587-591.
7. Oswald-Tranta B. "Thermo-inductive crack detection," *Nondestructive Testing and Evaluation*, vol. 22, 2007, pp. 137-153.
8. G. Zenzinger et al., "Thermographic crack detection by eddy current excitation," *Nondestructive Testing and Evaluation*, vol. 22, 2007, pp. 101-111.
9. McCullough R.W. "Transient thermographic technique for NDI of aerospace composite structures," *Thermosense XXVI, Apr 13-15 2004*, Orlando, FL, United States: The International Society for Optical Engineering, Bellingham, United States, 2004, pp. 390-402.
10. Maclachlan Spicer J. W., Kerns W. D., Aamodt L.C., Murphy J. C., "Time-Resolved Infrared Radiometry (TRIR) for Characterization of Impact Damage in Composite Materials," *Review of Progress in Quantitative NDE*, Thompson D.O. and Chimenti D.E. eds, Plenum **11A**: 433-440, 1998.
11. Giorleo G. and Meola C. "Comparison between Pulsed and Modulated Thermography in Glass-Epoxy Laminates", *NDT&E International*, vol. 35, pp. 287-292, 2002.
12. Zweschper T., Riegert G., Dillenz A. and Busse G. "Frequency modulated elastic wave thermography," *Proc. SPIE - The International Society for Optical Engineering, Thermosense XXV*, Orlando, FL, 2003*,* Eds. K. E. Cramer and X. P. Maldague, **5073**:386-391.
13. Busse G. "Optoacoustic Phase Angle Measurement for Probing a Metal", *Appl. Phys. Lett*., **35**:759–760, 1979
14. Ibarra-Castanedo C. and Maldague X. "Pulsed Phase Thermography Reviewed," *QIRT J.*, **1**(1):47-70, 2004.
15. Martin R. E., Gyekenyesi A. L., Shepard S. M., "Interpreting the Results of Pulsed Thermography Data," Materials Evaluation, **61**(5):611-616, 2003.
16. Pilla M., Klein M., Maldague X. and Salerno A., "New Absolute Contrast for Pulsed Thermography," QIRT 2002, D. Balageas, G. Busse, G. Carlomagno (eds.), *Proc. of QIRT*, pp. 53-58, 2002.

17. Ibarra-Castanedo C., Bendada A. and Maldague X. "Image and signal processing techniques in pulsed thermography," *GESTS Int'l Trans. Computer Science and Engr.,* **22**(1): 89-100, November 2005**a**.

18. Klein M., Pilla M. and Maldague X. "IR_View: A graphical user interface to process infrared images with MATLAB," application and documentation available online at: http://irview.m-klein.com (accessed February 21st 2007).

19. González D. A., Ibarra-Castanedo C., Madruga F. J. and Maldague X. "Differentiated absolute phase contrast algorithm for the analysis of pulsed thermographic sequences," ***Infrared Phys. Techn.,*** **48**:16-21, 2006.

20. Benítez H. D., Ibarra-Castanedo C., Bendada A., Maldague X. P. Loaiza H., Caicedo E. "Definition of a new thermal contrast and pulse correction for defect quantification in pulsed thermography," *Infrared Physics and Technology*, **51**(3):160-167, 2008.

21. Shepard S. M., Lhota J. R., Rubadeux B. A., Ahmed T., Wang D. "Enhancement and reconstruction of thermographic NDT data", *Proc. SPIE - The International Society for Optical Engineering, Thermosense XXIV*, Orlando, FL, 2002*,* Eds. X. P. Maldague and A. Rozlosnik, **4710**:531-535.

22. Shepard S. M. "Advances in Pulsed Thermography", *Proc. SPIE - The International Society for Optical Engineering, Thermosense XXVIII*, Orlando, FL, 2001*,* Eds. A. E. Rozlosnik and R. B. Dinwiddie, **4360**:511-515, 2001.

23. Rajic N. "Principal component thermography for flaw contrast enhancement and flaw depth characterization in composite structures," *Compos. Struct.*, **58**:521-528, 2002.

24. Marinetti S., Grinzato E., Bison P. G., Bozzi E. Chimenti M. Pieri G. and Salvetti O. "Statistical analysis of IR thermographic sequences by PCA," *Infrared Phys. & Technol*., **46**:85-91, 2004.

25. Maldague X. P. and Marinetti S. "Pulse Phase Infrared Thermography," *J. Appl. Phys.*, **79**(5):2694-2698, 1996.

26. Ibarra-Castanedo C. and Maldague X. "Pulsed Phase Thermography Reviewed," *QIRT J.*, **1**(1):47-70, 2004.

27. Ibarra-Castanedo C. "Quantitative subsurface defect evaluation by pulsed phase thermography: depth retrieval with the phase," *Ph. D. thesis*, Laval University, 2005. [accessible online: http://www.theses.ulaval.ca/2005/23016/23016.pdf].

28. Meola C. and Carlomagno G. M. "Recent Advances in the Use of Infrared Thermography", *Meas. Sci. Technol.*, **15**:27–58, 2004.

29. Madruga F. J., Ibarra-Castanedo C., Conde O. M, Maldague X. P. and Lopez-Higuera J. M "Enhanced contrast detection of subsurface defects by pulsed infrared thermography based on the fourth order statistic moment, kurtosis," *SPIE - The International Society for Optical Engineering, Thermosense XXXI*, Orlando, FL, April 13-17 2009*,* Eds. Douglas D. Burleigh and Ralph B. Dinwiddie, Paper **7299-28**.

30. Madruga F. J., Ibarra-Castanedo C., Conde O. M, Lopez-Higuera J. M and Maldague X. P. "Automatic data processing based on the skewness statistic parameter for subsurface defect detection by active infrared thermography," *Proc. QIRT 9 – Quantitative Infrared Thermography*, [CD-ROM], Krakow, Poland, July 2-5, 2008.